Biochemical and Biophysical Research Communications 461 (2015) 300–306

Contents lists available at ScienceDirect

Biochemical and Biophysical Research Communications

journal homepage: www.elsevier.com/locate/ybbrc

Two specific membrane-bound aminopeptidase N isoforms from *Aedes aegypti* larvae serve as functional receptors for the *Bacillus thuringiensis* Cry4Ba toxin implicating counterpart specificity

Aratee Aroonkesorn [a], Kusol Pootanakit [a], Gerd Katzenmeier [a], Chanan Angsuthanasombat [a, b, *]

[a] Bacterial Protein Toxin Research Cluster, Institute of Molecular Biosciences, Mahidol University, Salaya Campus, Nakornpathom 73170, Thailand
[b] Laboratory of Molecular Biophysics and Structural Biochemistry, Biophysics Institute for Research and Development (BIRD), Bangkok 10160, Thailand

ARTICLE INFO

Article history:
Received 25 March 2015
Available online 12 April 2015

Keywords:
Baculovirus expression system
Cry δ-endotoxin
Cytotoxicity assay
Membrane-bound APN
Double immunolocalization
APN structure

ABSTRACT

The interaction between *Bacillus thuringiensis* Cry toxins and their receptors on midgut cells of susceptible insect larvae is the critical determinant in toxin specificity. Besides GPI-linked alkaline phosphatase in *Aedes aegypti* mosquito-larval midguts, membrane-bound aminopeptidase N (AaeAPN) is widely thought to serve as a Cry4Ba receptor. Here, two full-length AaeAPN isoforms, AaeAPN2778 and AaeAPN2783, predicted to be GPI-linked were cloned and successfully expressed in *Spodoptera frugiperda* (*Sf*9) cells as 112- and 107-kDa membrane-bound proteins, respectively. In the cytotoxicity assay, *Sf*9 cells expressing each of the two AaeAPN isoforms showed increased sensitivity to the Cry4Ba mosquito-active toxin. Double immunolocalization revealed specific binding of Cry4Ba to each individual AaeAPN expressed on the cell membrane surface. Sequence analysis and homology-based modeling placed these two AaeAPNs to the M1 aminopeptidase family as they showed similar four-domain structures, with the most conserved domain II being the catalytic component. Additionally, the most variable domain IV containing negatively charged surface patches observed only in dipteran APNs could be involved in insect specificity. Overall results demonstrated that these two membrane-bound APN isoforms were responsible for mediating Cry4Ba toxicity against AaeAPN-expressed *Sf*9 cells, suggesting their important role as functional receptors for the toxin counterpart in *A. aegypti* mosquito larvae.

1. Introduction

Cry δ-endotoxins produced by Gram-positive spore-forming *Bacillus thuringiensis* (*Bt*) are highly toxic toward a wide range of insect larvae [1]. Of particular interest, the Cry4Ba toxin from *Bt* subsp. *israelensis* is specifically active against mosquito larvae of the genus *Aedes* and *Anopheles,* vectors of various human diseases including dengue fever, chikungunya, yellow fevers and malaria [2,3]. After ingestion by susceptible insect larvae, these Cry toxins which are produced as insoluble protoxins are solubilized in the larval midgut lumen (generally alkaline pH for dipteran and lepidopteran larvae) prior to their activation by gut proteases to yield ~65-kDa active toxins [2,4]. According to all the known Cry structures, the activated toxins consist of three distinct functional domains: an α-helical bundle (DI), a β-sheet prism (DII) and a β-sheet sandwich (DIII). DI and DII have been revealed as membrane-pore formation and receptor recognition, respectively [5]. Recently, we have demonstrated that charge-reversal mutations at Asp^{454} (D454R and D454K) located within a receptor-binding loop of Cry4Ba-DII markedly increases the toxin activity against less-susceptible *Culex* larvae, suggesting a role of the charged side-chain in determining target specificity [6].

A number of activated Cry toxins are shown to bind to a variety of specific receptors located on the midgut epithelium cells [7]. This toxin-receptor interaction would promote toxin oligomerization and membrane-pore formation, resulting in midgut cell lysis and the eventual death of the target larvae [7]. Specific binding to their individual receptors is believed to be the critical determinant in Cry

Abbreviations: AaeAPN, *Aedes aegypti* membrane-bound aminopeptidase N; AeaALP, *Aedes aegypti* membrane-bound alkaline phosphatase; CAT, chloramphenicol acetyltransferase; GPI, glycosylphosphatidylinositol.

* Corresponding author. Bacterial Protein Toxin Research Cluster, Institute of Molecular Biosciences, Mahidol University, Salaya Campus, Nakornpathom 73170, Thailand.
E-mail address: chanan.ang@mahidol.ac.th (C. Angsuthanasombat).

http://dx.doi.org/10.1016/j.bbrc.2015.04.026
0006-291X/

toxin specificity. In mosquito larvae, various membrane-bound proteins were identified as functional receptors for several Cry toxins, including *Aedes* and *Anopheles* cadherin-like proteins for Cry11Aa and Cry4Ba, respectively [8,9], *Aedes* alkaline phosphatases (ALP) for Cry11Aa and Cry4Ba [10–12], *Anopheles* ALP for Cry11Ba [13], *Aedes* aminopeptidases N (APN) for Cry4Ba and Cry11Aa [14,15] and *Anopheles* APN for Cry11Ba [16,17]. Recently, the Cyt2Aa toxin from *Bt* subsp. *darmstadiensis* has also been reported as another binding protein for Cry4Ba to exert synergistic toxicity against *Aedes aegypti* larvae [18]. However, the structural basis for Cry4Ba toxin-receptor interaction is still unclear and need to be explored.

The APN family is a class of M1 zinc-metalloprotease/peptidase superfamily that cleaves neutral amino acids from the N-terminus of polypeptides [19]. Members of this family are classified as gluzincins that contain a consensus Zn^{2+}-binding sequence [HEXXH-(X18)-E, where X stands for any amino acid] and a GAMEN sequence in the active site [19]. To date, crystal structures of the M1 superfamily are available for various species, *e.g. Escherichia coli* (PDB ID: 2HPT), *Plasmodium falciparum* (PDB ID: 3EBG), *Thermoplasma acidophilum* (PDB ID: 1Z5H) and human (PDB ID: 2YD0) [20]. They all show similar overall structures, with domain II being the most conserved and domain IV the most variable [21]. In addition to being studied for their typical role in digestion, APNs have also been extensively studied as tumor-related targets, receptors for coronavirus and bacterial toxins [21,7].

Previously, we have demonstrated in *A. aegypti* mosquito larvae that knockdown of three different GPI-anchored APN isoforms (AaeAPN2778, AaeAPN2783 and AaeAPN5808) *via* RNA interference resulted in the decrease of Cry4B toxicity [14]. Here, we provide further insights into the molecular structure and specific binding to the Cry4Ba toxin of two functionally expressed AaeAPN isoforms, AaeAPN2778, AaeAPN2783, on the *Sf*9 insect cell membrane.

2. Materials and methods

2.1. Amplification of GPI-anchored APN-coding regions from A. aegypti larval midgut cDNA

Three pairs of AaeAPN-specific primers were designed (*see* Supplementary Table 1) based on three putative GPI-anchored APN sequences from *A. aegypti* genome database (www.vectorbase.org): AaeAPN2778, AaeAPN2783 and AaeAPN5808, where the numbering is referred to the last four digits (underlined) of transcript identification from VectorBase (AAEL012778-RA, AAEL012783-RA and AAEL005808-RA). Then, potential GPI-anchoring sites were predicted by four different GPI-prediction programs: PredGPI (gpcr2.biocomp.unibo.it/gpipe/pred.htm), big-PI Predictor (mendel.imp.univie.ac.at/sat/gpi/gpi_server.html), FragAnchor (http://navet.ics.hawaii.edu/~fraganchor/NNHMM/NNHMM.html) and GPI-SOM (http://gpi.unibe.ch/). Signal peptide and N-glycosylation sites were further predicted by SignalP and NetNGlyc1.0 Server (http://www.cbs.dtu.dk/services/NetNGlyc/), respectively.

First-strand cDNA was synthesized from RNA transcripts of the 5th instar *A. aegypti* larval midgut using oligo-dT primer. Coding sequences of these three AaeAPNs were individually amplified *via* the cDNA product with Phusion DNA polymerase (Finnzymes). The expected size-amplicons were purified, ligated to the pENTR/SD-TOPO vector and transformed into One-Shot TOP10 competent cells, following the manufacturer's protocol (Invitrogen). Recombinant pENTR/AaeAPN plasmids were randomly selected and their sequences verified by DNA sequencing.

2.2. Transient expression of recombinant AaeAPN isoforms in insect cells

Each of recombinant pENTR/AaeAPN plasmids was selected for an *in vitro* Lamda Recombination (LR). Individual AaeAPN fragments were transferred from pENTR/AaeAPN plasmids to Baculodirect Linear DNA (Invitrogen) by site-specific recombination. Briefly, ~200 ng of pENTR/AeAPN plasmids were mixed with Baculodirect C-term Linear DNA (~200 ng) and LR Clonase II for 18 h at 26 °C. The recombinant AaeAPN expression vectors were subsequently transfected into the insect *Sf*9 (*Spodoptera frugiperda* 9) cells using Cellfectin, following manufacturer's protocol (Invitrogen).

2.3. Mass spectrometry (MS) analysis of AaeAPNs proteins

Cell lysates collected from *Sf*9 cells expressing each recombinant AaeAPN were separated by SDS-PAGE. The protein bands corresponding to AaeAPN proteins were excised from the gel and subjected to liquid chromatography-mass spectrometry (LC-MS) analysis (MaXis, Bruker).

2.4. Expression and preparation of the Cry4Ba active toxin

Cry4Ba-R203Q mutant toxin (one tryptic cleavage site was eliminated by substitution at Arg^{203} with Gln) which still retains high larvicidal activity [22] was used in this study. *E. coli* strain JM109 expressing the R203Q mutant was grown in LB medium containing 100 μg/mL ampicillin at 37 °C until OD_{600} reached 0.3–0.6. Toxin expression was induced with 0.1 mM isopropyl-β-D thiogalactopyranoside for 4 h and harvested by centrifugation at 6000× *g*. The cell pellet was re-suspended in 100 mM KH_2PO_4 (pH 5.0) containing 0.1% Triton X-100 and 0.5% NaCl, and further disrupted by sonication (VCX750-Sonics Vibra Cell™) with the following parameters: 5 cycles of amplitude 60%, 10-s ON, 30-s OFF with a total time ON = 1 min/cycle. Protein inclusions were collected by centrifugation at 6000× *g*, washed and subsequently re-suspended in distilled water. The concentration of the partially purified inclusion was determined using the Bradford-based protein microassay. Cry4Ba toxin inclusions were solubilized in carbonate buffer (50 mM Na_2CO_3/$NaHCO_3$, pH 9.0) at a final concentration of 1 mg/mL for 1 h at 37 °C. The solubilized toxin was activated by trypsin (tolylsulfonyl phenylalanyl chloromethyl ketone-treated trypsin; Sigma) at a ratio of 1:10 enzyme/toxin (w/w). The 65-kDa activated toxin was further purified by size-exclusion chromatography (Superose 12 10/300, GE Healthcare) and eluted with the carbonate buffer (pH 9.0) at a flow rate of 0.4 mL/min. The purified Cry4Ba protein fraction was then concentrated with a 10-kDa-MWCO Millipore membrane (Merck KGaA) and analyzed by SDS-PAGE.

2.5. Cytotoxicity assays of the Cry4Ba toxin on Sf9 cells-expressing AaeAPNs

100 μg/mL of Cry4Ba toxin (mixed with 1 mL Sf-900 medium (Invitrogen) was applied to the 5-day post-infected *Sf*9 cells expressing recombinant AaeAPNs, AaeALP (*Aedes* membrane-bound alkaline phosphatase) and CAT control (chloramphenicol acetyltransferase) at ~8×10^5 cells/mL in a 6-well culture plate and further incubated at 26 °C for 2 h. The cell morphology was observed under light microscope. To determine viability of cells, PrestoBlue™ cell viability assay (Life Technologies, USA) was performed. Briefly, 100 μL PrestoBlue™ reagent was added directly to cells in 900 μL culture medium, incubated for 10 min at 37 °C and then spectrofluorometrically quantitated (excitation at 530 nm;

emission at 590 nm). The significance of the data between samples was analyzed using Student's *t*-test.

2.6. Double immunofluorescence staining of the Cry4Ba toxin and AaeAPNs

Interactions between the Cry4Ba toxin and AaeAPNs were investigated by double immunofluorescence staining. After 5-day post-infection, *Sf9* cells expressing AaeAPNs (AaeAPN2778 or AaeAPN2783), CAT or AaeALP were incubated with 100 μg/mL of the activated Cry4Ba toxin at 26 °C for 2 h. Cells were washed twice with PBS and collected by centrifugation at 3000× *g*. The cell pellets were fixed with 4% paraformaldehyde in PBS buffer and then blocked with 3% BSA followed by 1-h incubation with primary antibodies, either mouse monoclonal antibody-2F(1H2) specific to the Cry4Ba domain III at 1:100 dilution or rabbit polyclonal antibodies against human APN (anti-CD13, ab9389, Abcam) at 1:50 dilution. The cells were rinsed twice with PBS and collected by centrifugation, followed by another 1-h incubation with secondary antibodies, either FITC-conjugated rabbit anti-mouse IgG (Jackson Immuno Research) or Alexa Fluor® 647-conjugated goat anti-rabbit IgG antibody (Thermo Fisher Scientific) at 1:100 dilution. The unbound conjugate was removed by washing with PBS. The stained cells were collected by centrifugation and deposited on the glass slide and mounted with a coverslip. The immuno-stained cells were then examined on a confocal laser scanning microscope (Olympus FV1000).

2.7. Homology-based modeling of AaeAPN isoforms

Plausible homology models of AaeAPN2778 and AaeAPN2783 were constructed using SWISS-MODEL, a protein structure homology-modeling server (http://swissmodel.expasy.org/). For template protein identification, the homologous structure was identified by searching the Protein Data Bank (PDB) using BLAST algorithm (http://www.rcsb.org/). ClustalW program was employed to identify conserved and variable regions between these two AaeAPNs and the template proteins. After manual adjustment, alignment files were subjected to SWISS-MODEL server in alignment mode. Stereochemical quality and Ramachandran plot analyses of both AaeAPN models were performed using QMEAN [23] and RAMPAGE [24] servers.

3. Results and discussion

3.1. Typical characteristics of membrane-bound APN isoforms from A. aegypti larval midgut

Membrane-bound APNs have been identified as Cry toxin receptors in various species of insect larvae such as *Bombyx mori, Heliothis virescens, Ostrinia nubilalis* and *Manduca sexta* [25–28]. In *Anopheles* and *Aedes* mosquito larvae, several APNs were also identified as putative receptors for the Cry4Ba, Cry11Aa and Cry11Ba toxins [14–16]. Here, three different full-length genes encoding AaeAPN2778, AaeAPN2783 and AaeAPN5808 were cloned from *A. aegypti* larval midgut RNA transcripts with specific primers using RT-PCR strategy. The PCR products obtained were of the expected sizes, *i.e.* 3003-bp for AaeAPN2778, 2868-bp for AaeAPN2783 and 2848-bp for AaeAPN5808 (Fig. 1, *inset*). The translated cDNA sequences of AaeAPN2778, AaeAPN2783 and AaeAPN5808 revealed open reading frames of 1000, 955 and 947 amino acid residues (*see* Supplementary Fig. 1) with a predicted molecular mass of 112, 107 and 108 kDa, respectively. The APN conserved sequences, HEXXH_E and GAMEN sequences [19] were identified in all three AaeAPN clones, indicating that these three AaeAPNs belonged to the member of M1 zinc-metalloprotease/peptidase superfamily. Moreover, these three AaeAPNs also contained a putative N-terminal signal peptide together with their predicted GPI-anchored sites on the C-terminus (Fig. 1) that strongly suggested these AaeAPNs as membrane-bound proteins attached to the cell surface *via* a GPI-anchor.

To generate the recombinant AaeAPN proteins, baculovirus expression was performed. The infected *Sf9* cells were harvested after 5 days for protein expression analysis. Both AaeAPN2778 and AaeAPN2783 were detected as dominant protein bands with sizes corresponding to the predicted mass of 112 and 107 kDa, respectively (Fig. 2C). For the controls, 30-kDa and 58-kDa protein bands were observed as expected for CAT and AaeALP-expression, respectively (Fig. 2C). However, no protein of the expected size was found for AaeAPN5808. Thus, the specific toxin-receptor interaction study (*see* below) employed only the 112-kDa AaeAPN2778 and the 107-kDa AaeAPN2783.

Further analysis by LC-MS confirmed that the 112- and 107-kDa protein bands indeed represent the expressed products of AaeAPN2778 and AaeAPN2783, respectively; multiple peptide sequences were found to correspond to both AaeAPN2778 (^{165}RLSNSEDGFYISSYVNKD^{182}, ^{524}RRTYETGDIIISQERF^{539}, ^{791}RSMII-SALGCSENKQ^{805}) and AaeAPN2783 (^{92}RQITVTHVKL^{101}, ^{280}KVINA-LEDYLQVKY^{293}, ^{743}KDIDPNLKG^{751}, ^{831}RVGLETAMKFLDANAATIDR LYNGGSFGGRA^{861}). It is noteworthy that the size of the expressed protein bands correspond to the predicted 112-kDa AaeAPN2778 and 107-kDa AaeAPN2783, suggesting that the recombinant APN proteins were not glycosylated, at least, in the *Sf9* cells. This finding was similar to another Cry4Ba receptor, *i.e.* AaeALP, which is found not to be glycosylated in *Sf9* cells [12] and is functionally expressed in *E. coli* [29]. Also, another dipteran APN from *Anopheles* mosquito-larvae (AgAPN2) expressed in *E. coli* was shown not to have glycosylation for Cry11Ba binding [17] unlike some identified lepidopteran APNs that need the sugar moiety for binding to their toxin counterparts [7,28].

3.2. Cytotoxic effect and binding of the Cry4Ba toxin mediated by individual AaeAPN isoforms

In vitro cytotoxicity assays were carried out to test whether the two recombinant AaeAPN isoforms can serve as a functional receptor for the Cry4Ba toxin. It was found that when Cry4Ba (100 μg/mL) was added, *Sf9* cells expressing AaeAPN2778, AaeAPN2783 or AaeALP appeared to undergo cell lysis as visualized under light microscope (Fig. 2A). To quantitate this observation, cell viability assay was performed. The result showed an increase in percent mortality of *Sf9* cells expressing AaeAPN2778 (35.0 ± 4.5%) and AaeAPN2783 (27.0 ± 2.2%) when compared to the control *Sf9* cells expressing CAT (10.0 ± 0.8% cell mortality) (Fig. 2B). Cell mortality mediated by these two AaeAPNs was similar to AaeALP (31.7 ± 2.8% cell mortality) which has been previously identified as a Cry4Ba receptor [12], suggesting that both AaeAPN2778 and AaeAPN2783, like AaeALP, share a common role as a toxin receptor mediating the Cry4Ba cytotoxicity. Moreover, this result was in agreement with our previous study that AaeAPN2778- or AaeAPN2783-knockdown larvae became less susceptible to the Cry4Ba toxin [14], strongly suggesting that these two APN isoforms serve as functional receptors for the Cry4Ba toxin in *A. aegypti* mosquito-larvae.

Further studies *via* double-labeling immunofluorescence experiments showed that Cry4Ba-immunoreactivity was seen in AaeAPNs- and AaeALP-expressing *Sf9* cells but not in CAT-expressing cells (Fig. 3). Both the Cry4Ba toxin and AaeAPNs were detected on the cell membrane surface with extensive co-localization (Fig. 3***I*** and ***L***), indicating that Cry4Ba was able to bind only to *Sf9* cells-expressing membrane-bound AaeAPNs or

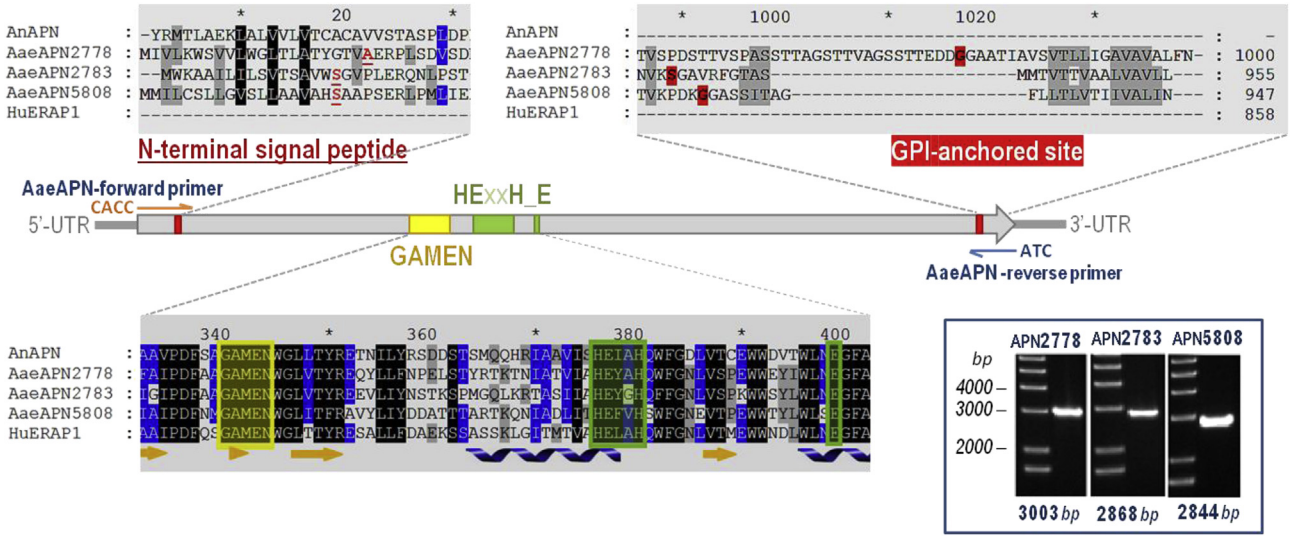

Fig. 1. Multiple sequence alignments of the deduced amino acid sequences of AaeAPN2778, AaeAPN2783 and AaeAPN5808 against APNs from *An. gambiae* mosquito-larvae–AgAPN [17] and human–HuERAP1 [20]. HuERAP1 is used as the reference sequence denoting secondary structure elements. The conserved GAMEN and gluzincin sequences involved in Zn^{2+}-binding or substrate-binding are boxed in yellow and green, respectively. The predicted N-terminal signal peptide is underlined; the putative GPI-anchor site is highlighted in red. Inset is RT-PCR analysis of total RNAs from *A. agypti* larval midguts, showing the cDNAs of all three full-length transcripts as their sizes indicated on each lane. (For interpretation of the references to color in this figure legend, the reader is referred to the web version of this article.)

AaeALP. These results also suggested that both AaeAPN isoforms were expressed in *Sf*9 cells as membrane-bound proteins. Taken altogether with the cytotoxicity results suggest that specific binding of Cry4Ba to its single counterpart (AaeAPN2778 or AaeAPN2783) is sufficient for mediating the toxin activity against individual receptor-expressing *Sf*9 cells without the need of pre-interaction with another receptor. Nevertheless, it has been shown both in *vivo* and *in vitro* for lepidopteran-specific Cry1A toxins that pre-binding of the toxin to cadherin-like receptors is required for toxin oligomerization prior to interacting with second membrane-bound receptors (*e.g.* APNs or ALPs) for insertion and pore formation [7,30].

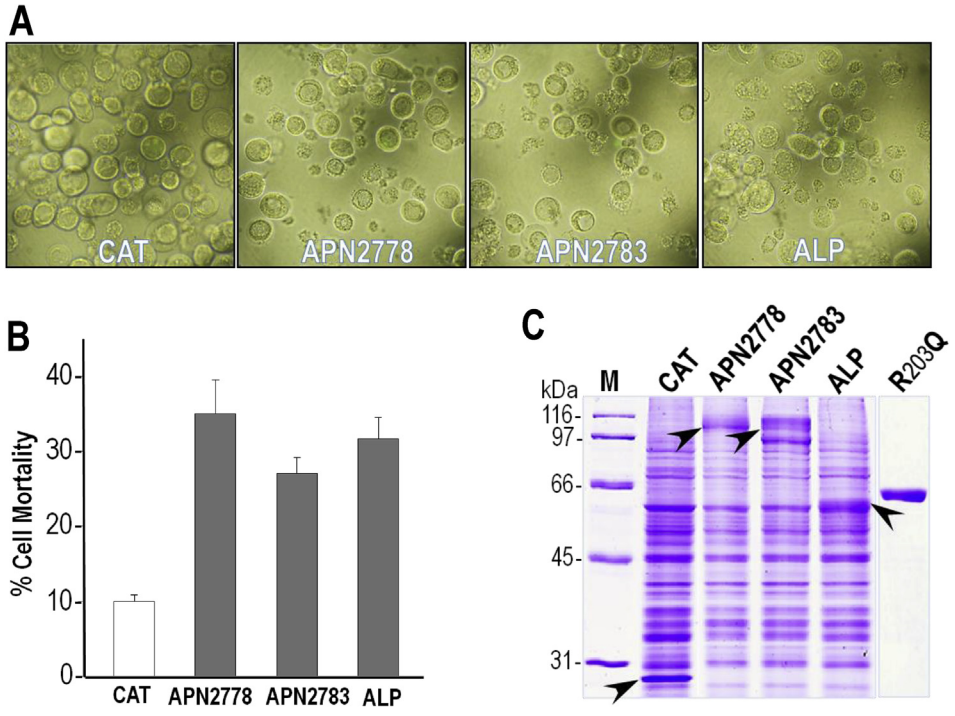

Fig. 2. Cytotoxicity of Cry4Ba against AaeAPNs expressing *Sf*9 cells. (**A**) Representative light micrographs of *Sf*9 cells expressing, from left to right, CAT, AaeAPN2778, AaeAPN2783 and AaeALP, incubated with 100 μg/mL Cry4Ba-R203Q for 2 h. (**B**) Percent cell mortality, as assayed using PrestoBlue, of *Sf*9 cells expressing CAT, AaeAPN2778, AaeAPN2783 or AaeALP. Bars denote standard errors of the mean from three independent experiments each performed in triplicates. Shaded graphs represent mortality (%) of the treated cells expressing AaeAPN2778, AaeAPN2783 or AaeALP that are significantly different (p values < 0.05) from that of the CAT-control cells. (**C**) SDS-PAGE analysis (12% gel) of *Sf*9 cell lysates containing CAT, AaeAPN2778, AaeAPN2783 or AaeALP (arrowed), and of the Cry4Ba-R203Q toxin after trypsin activation. M, broad-range protein markers.

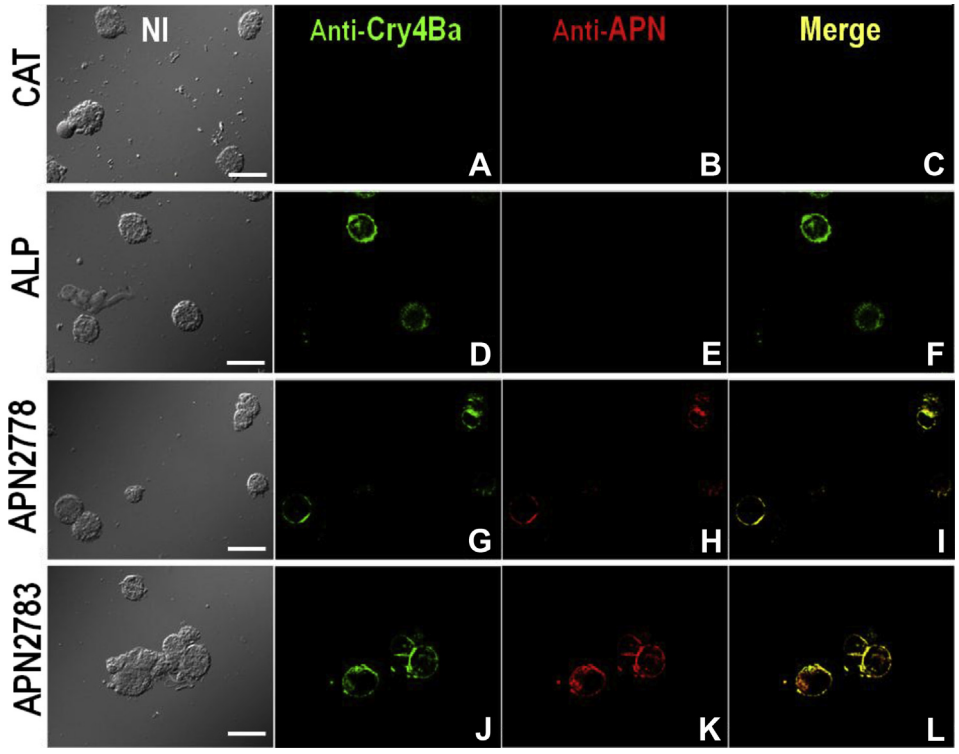

Fig. 3. Immunocolocalization of the Cry4Ba toxin and AaeAPNs on *Sf9* cells expressing AaeAPNs. *Sf9* cells expressing CAT, AaeALP, AaeAPN2778 or AaeAPN2783 were treated with Cry4Ba-R203Q (100 μg/mL) for 2 h prior to being fixed with 4% paraformaldehyde, blocked, and incubated with antibodies against the Cry4Ba toxin or human APN (anti-CD13), followed by secondary antibodies conjugated with FITC (green) and Alexa Fluor® 647 (red), respectively. Cry4Ba bindings can be seen as FITC (green) fluorescent signal (***A***, ***D***, ***G*** and ***J***) while AaeAPN expression can be seen as Alexa Fluor® 647 (red) fluorescent signal (***B***, ***E***, ***H*** and ***K***). Merged images from the two fluorescent channels are shown in ***C***, ***F***, ***I*** and ***L***. NI is the Nomarski interference contrast view. Scale bar is 20 μm. (For interpretation of the references to color in this figure legend, the reader is referred to the web version of this article.)

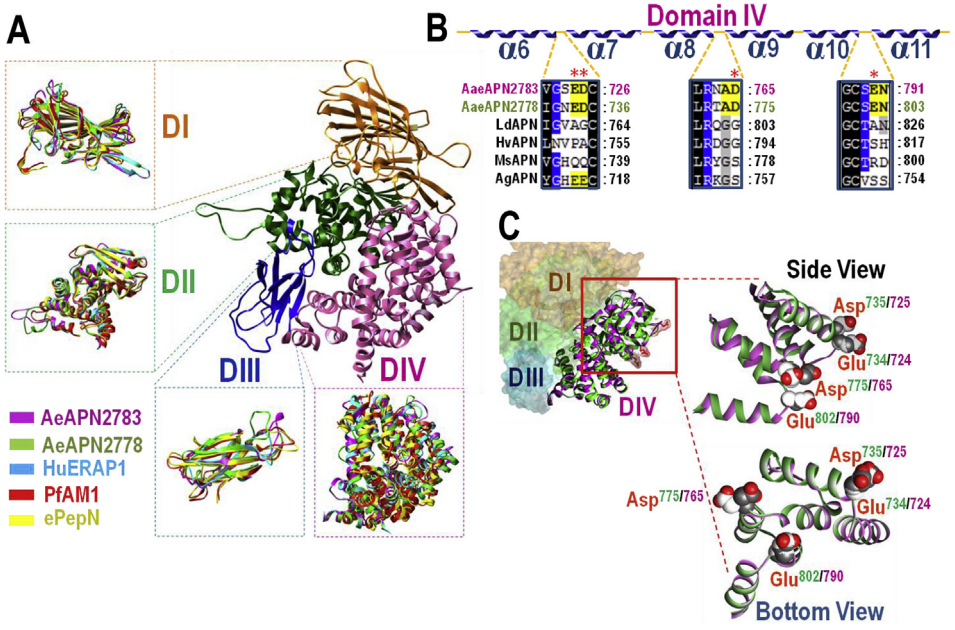

Fig. 4. 3D-modeled structures of AaeAPN2783 and AaeAPN2778. (**A**) Domain organization and superimposition of plausible 3D structures of AaeAPN2778 (light green) and AaeAPN2783 (magenta) as compared to others known APN structures in the M1 super family: HuERAP1, (PDB 2YD0: light blue), PfAM1 (PDB 3EBG: red) and ePepN (PDB 2HPT: yellow). AaeAPN2783 is used as a representative structure for domain division; domain I (DI, orange), domain II (DII, green), domain III (DIII, dark blue) and domain IV (DIV, magenta). (**B**) Multiple alignments of three-loop sequences between α6-α7, α8-α9 and α10-α11 within the toxin-binding domain IV of both AaeAPN2778 and AaeAPN2783 with those of *An. gambiae* mosquito-APN and three other lepidopteran APNs (*i.e.*, *L. dispar* APN, *H. virescens* APN and *M. sexta* APN) revealing conserved-negatively charged residues (indicated by *) of AaeAPN2778 and AaeAPN2783 (AaeAPN2778: Glu^{734}, Asp^{735}, Asp^{775} and Glu^{802}; AaeAPN2783: Glu^{724}, Asp^{725}, Asp^{765} and Glu^{790}). (**C**) Superimposition of AaeAPN2778-domain IV (shaded green/grey) and AaeAPN2783-domain IV (shaded magenta/white) structures revealing negatively charged patches on the surface exposed loops. All structures were generated by using UCSF Chimera program. (For interpretation of the references to color in this figure legend, the reader is referred to the web version of this article.)

3.3. Common structural features of AaeAPN isoforms and implications for specific interactions

Currently, there is no three-dimensional (3D) structure of insect APNs, homology-based models of AaeAPNs were therefore built based on the highest sequence similarity. Human endoplasmic reticulum aminopeptidase 1 (PDB 2YD0) [20] was therefore selected as a template for homology modeling as it showed the highest similarity with 50% and 46% to AaeAPN2778 and AaeAPN2783, respectively. To validate the models, the stereochemical quality of AaeAPN2778 and AaeAPN2783 showed the overall QMEAN score of 0.609 and 0.591, respectively, suggesting good quality models as estimated model reliability is between 0 and 1, with higher values for more reliable structures [23]. In addition, Ramachandran plot analysis revealed that 97.3% and 97.6% of AaeAPN2778 and AaeAPN2783 amino acid residues, respectively, are present in the most favored and additional allowed positions [24], suggesting that both 3D-modeled structures are mostly in the sterically favorable main-chain conformations.

When compared to the X-ray structure of other members of the M1 superfamily including *E. coli* APN (ePepN, PDB ID: 2HPT), *P. falciparum* APN (PfAM1, PDB ID: 3EBG) and human endoplasmic reticulum APN (HuERAP1, PDB ID: 2YD0) [20], the two AaeAPNs show overall structures similar to these known APN structures consisting of four structural domains: a β-sandwich (domain I), a thermolysin-like αβ fold (the most conserved domain II), a small β-sandwich (domain III) and an α-helical bundle (domain IV) (Fig. 4A). This suggests that AaeAPNs displayed high structural conservation among the M1 aminopeptidase family. It should be noted that in the most variable domain IV there is no predicted N-/O-glycosylation site in the Thr-rich C-terminal stalk regions (*see* Supplementary Fig. 1) which are believed to be a part of Cry1A-binding regions for the lepidopteran APNs [7], suggesting different toxin-binding sites between lepidopteran- and mosquito-APNs. Interestingly, when compared the variable domain IV of these two AaeAPNs among insect APNs that have been reported as Cry toxin receptors including *Lymantria dispar* APN [31], *M. sexta* APN [32], *H. virescens* APN [26] and *An. gambiae* APN [17], the conserved negatively charged residues were found only on the two AaeAPNs: Glu^{734}, Asp^{735}, Asp^{775} and Glu^{802} for AaeAPN2778; and Glu^{724}, Asp^{725}, Asp^{765} and Glu^{790} for AaeAPN2783 (*see* Fig. 4B, as indicated by *). These conserved-negatively charged patches placed them on the surface-exposed loops of both AaeAPN structures (Fig. 4C), possibly being involved in binding to the Cry4Ba toxin *via* ionic interactions and hence determining target specificity against *Aedes* larvae. Further studies, to better understand more critical insights into Cry4Ba toxin-receptor interactions, charged reversed mutagenesis on these putative interaction sites would be of great interest. Likewise, point mutations to positively charged side-chains on receptor-binding loop regions of the Cry4Ba toxin itself might perhaps improve the toxin activity and specificity against *Aedes* larvae, consistent with previous findings that Cry4Ba-charged-reversal mutants (D454R and D454K) exhibit increased binding affinity and larval toxicity to *Culex* larvae [6].

Conflict of interest

There are no conflicts of interest to declare.

Acknowledgments

This work was supported in part by grants from the Thailand Research Fund (IRG-57-8-0009 and BRG-53-8-0007). A PhD scholarship from the Development and Promotion of Science and Technology Talents Project (to A.A.) is gratefully acknowledged.

Appendix A. Supplementary data

Supplementary data related to this article can be found at http://dx.doi.org/10.1016/j.bbrc.2015.04.026.

Transparency document

Transparency document related to this article can be found online at http://dx.doi.org/10.1016/j.bbrc.2015.04.026.

References

[1] E. Schnepf, N. Crickmore, J. Van Rie, D. Lereclus, J. Baum, J. Feitelson, D.R. Zeigler, D.H. Dean, *Bacillus thuringiensis* and its pesticidal crystal proteins, Microbiol. Mol. Biol. Rev. 62 (1998) 775–806.
[2] C. Angsuthanasombat, Structural basis of pore formation by mosquito-larvicidal proteins from Bacillus thuringiensis, Open Toxinol J. (2010) 119–125.
[3] E. Ben-Dov, *Bacillus thuringiensis subsp. israelensis* and its dipteran-specific toxins, Toxins 6 (2014) 1222–1243.
[4] J. Carroll, M.G. Wolfersberger, D.J. Ellar, The *Bacillus thuringiensis* Cry1Ac toxin-induced permeability change in *Manduca sexta* midgut brush border membrane vesicles proceeds by more than one mechanism, J. Cell. Sci. 110 (1997) 3099–3104.
[5] P. Boonserm, P. Davis, D.J. Ellar, J. Li, Crystal structure of the mosquito-larvicidal toxin Cry4Ba and its biological implications, J. Mol. Biol. 348 (2005) 363–382.
[6] S. Visitsattapongse, S. Sakdee, S. Leetacheewa, C. Angsuthanasombat, Single-reversal charge in the β10-β11 receptor-binding loop of *Bacillus thuringiensis* Cry4Aa and Cry4Ba toxins reflects their different toxicity against *Culex* spp. larvae, Biochem. Biophys. Res. Commun. 450 (2014) 948–952.
[7] C.R. Pigott, D.J. Ellar, Role of receptors in *Bacillus thuringiensis* crystal toxin activity, Microbiol. Mol. Biol. Rev. 71 (2007) 255–281.
[8] J. Chen, K.G. Aimanova, L.E. Fernandez, A. Bravo, M. Soberon, S.S. Gill, *Aedes aegypti* cadherin serves as a putative receptor of the Cry11Aa toxin from Bacillus thuringiensis subsp. israelensis, Biochem. J. 424 (2009) 191–200.
[9] G. Hua, R. Zhang, M.A. Abdullah, M.J. Adang, *Anopheles gambiae* cadherin AgCad1 binds the Cry4Ba toxin of *Bacillus thuringiensis israelensis* and a fragment of AgCad1 synergizes toxicity, Biochemistry 47 (2008) 5101–5110.
[10] L.E. Fernandez, K.G. Aimanova, S.S. Gill, A. Bravo, M. Soberon, A GPI-anchored alkaline phosphatase is a functional midgut receptor of Cry11Aa toxin in *Aedes aegypti* larvae, Biochem. J. 394 (2006) 77–84.
[11] L.E. Fernandez, C. Martinez-Anaya, E. Lira, J. Chen, A. Evans, S. Hernandez-Martinez, H. Lanz-Mendoza, A. Bravo, S.S. Gill, M. Soberon, Cloning and epitope mapping of Cry11Aa-binding sites in the Cry11Aa-receptor alkaline phosphatase from *Aedes aegypti*, Biochemistry 48 (2009) 8899–8907.
[12] M. Dechklar, K. Tiewsiri, C. Angsuthanasombat, K. Pootanakit, Functional expression in insect cells of glycosylphosphatidylinositol-linked alkaline phosphatase from *Aedes aegypti* larval midgut: a *Bacillus thuringiensis* Cry4Ba toxin receptor, Insect Biochem. Mol. Biol. 41 (2011) 159–166.
[13] G. Hua, R. Zhang, K. Bayyareddy, M.J. Adang, *Anopheles gambiae* alkaline phosphatase is a functional receptor of *Bacillus thuringiensis jegathesan* Cry11Ba toxin, Biochemistry 48 (2009) 9785–9793.
[14] S. Saengwiman, A. Aroonkesorn, P. Dedvisitsakul, S. Sakdee, S. Leetachewa, C. Angsuthanasombat, K. Pootanakit, In vivo identification of *Bacillus thuringiensis* Cry4Ba toxin receptors by RNA interference knockdown of glycosylphosphatidylinositol-linked aminopeptidase N transcripts in *Aedes aegypti* larvae, Biochem. Biophys. Res. Commun. 407 (2011) 708–713.
[15] J. Chen, K.G. Aimanova, S. Pan, S.S. Gill, Identification and characterization of *Aedes aegypti* aminopeptidase N as a putative receptor of *Bacillus thuringiensis* Cry11A toxin, Insect Biochem. Mol. Biol. 39 (2009) 688–696.
[16] M.A. Abdullah, A.P. Valaitis, D.H. Dean, Identification of a *Bacillus thuringiensis* Cry11Ba toxin-binding aminopeptidase from the mosquito, *Anopheles quadrimaculatus*, BMC Biochem. 7 (2006) 16.
[17] R. Zhang, G. Hua, T.M. Andacht, M.J. Adang, A 106-kDa aminopeptidase is a putative receptor for *Bacillus thuringiensis* Cry11Ba toxin in the mosquito *Anopheles gambiae*, Biochemistry 47 (2008) 11263–11272.
[18] C. Lailak, T. Khaokhiew, C. Promptmas, B. Promdonkoy, K. Pootanakit, C. Angsuthanasombat, *Bacillus thuringiensis* Cry4Ba toxin employs two receptor-binding loops for synergistic interactions with Cyt2Aa2, Biochem. Biophys. Res. Commun. 435 (2013) 216–221.
[19] N.M. Hooper, Families of zinc metalloproteases, FEBS Lett. 354 (1994) 1–6.
[20] G. Kochan, T. Krojer, D. Harvey, R. Fischer, L. Chen, M. Vollmar, F. von Delft, K.L. Kavanagh, M.A. Brown, P. Bowness, P. Wordsworth, B.M. Kessler, U. Oppermann, Crystal structures of the endoplasmic reticulum aminopeptidase-1 (ERAP1) reveal the molecular basis for N-terminal peptide trimming, Proc. Natl. Acad. Sci. U. S. A. 108 (2011) 7745–7750.
[21] T.T. Nguyen, S.-C. Chang, I. Evnouchidou, I.A. York, C. Zikos, K.L. Rock, A.L. Goldberg, E. Stratikos, L.J. Stern, Structural basis for antigenic peptide precursor processing by the endoplasmic reticulum aminopeptidase ERAP1, Nat. Struct. Mol. Biol. 18 (2011) 604–613.

[22] N. Thamwiriyasati, S. Sakdee, P. Chuankhayan, G. Katzenmeier, C.J. Chen, C. Angsuthanasombat, Crystallization and preliminary X-ray crystallographic analysis of a full-length active form of the Cry4Ba toxin from *Bacillus thuringiensis*, Acta Crystallogr. Sect. F. Struct. Biol. Cryst. Commun. 66 (2010) 721–724.
[23] P. Benkert, S.C. Tosatto, D. Schomburg, QMEAN: a comprehensive scoring function for model quality assessment, Proteins 71 (2008) 261–277.
[24] S.C. Lovell, I.W. Davis, W.B. Arendall 3rd, P.I. de Bakker, J.M. Word, M.G. Prisant, J.S. Richardson, D.C. Richardson, Structure validation by Cα geometry: phi,psi and Cβ deviation, Proteins 50 (2003) 437–450.
[25] S. Atsumi, E. Mizuno, H. Hara, K. Nakanishi, M. Kitami, N. Miura, H. Tabunoki, A. Watanabe, R. Sato, Location of the *Bombyx mori* aminopeptidase N type 1 binding site on *Bacillus thuringiensis* Cry1Aa toxin, Appl. Environ. Microbiol. 71 (2005) 3966–3977.
[26] S.S. Gill, E.A. Cowles, V. Francis, Identification, isolation, and cloning of a *Bacillus thuringiensis* CryIAc toxin-binding protein from the midgut of the lepidopteran insect *Heliothis virescens*, J. Biol. Chem. 270 (1995) 27277–27282.
[27] C.M. Crava, Y. Bel, S.F. Lee, B. Manachini, D.G. Heckel, B. Escriche, Study of the aminopeptidase N gene family in the lepidopterans *Ostrinia nubilalis* (Hubner) and *Bombyx mori* (L.): sequences, mapping and expression, Insect Biochem. Mol. Biol. 40 (2010) 506–515.
[28] P.J. Knight, J. Carroll, D.J. Ellar, Analysis of glycan structures on the 120 kDa aminopeptidase N of *Manduca sexta* and their interactions with *Bacillus thuringiensis* Cry1Ac toxin, Insect Biochem. Mol. Biol. 34 (2004) 101–112.
[29] A. Thammasittirong, M. Dechklar, S. Leetachewa, K. Pootanakit, C. Angsuthanasombat, *Aedes aegypti* membrane-bound alkaline phosphatase expressed in *Escherichia coli* retains high-affinity binding for Bacillus thuringiensis Cry4Ba toxin, Appl. Environ. Microbiol. 77 (2011) 6836–6840.
[30] L. Portugal, J.L. Gringorten, G.F. Caputo, M. Soberon, C. Munoz-Garay, A. Bravo, Toxicity and mode of action of insecticidal Cry1A proteins from *Bacillus thuringiensis* in an insect cell line, CF-1, Peptides 53 (2014) 292–299.
[31] K.J. Garner, S. Hiremath, K. Lehtoma, A.P. Valaitis, Cloning and complete sequence characterization of two gypsy moth aminopeptidase-N cDNAs, including the receptor for *Bacillus thuringiensis* Cry1Ac toxin, Insect Biochem. Mol. Biol. 29 (1999) 527–535.
[32] P.J. Knight, B.H. Knowles, D.J. Ellar, Molecular cloning of an insect aminopeptidase N that serves as a receptor for *Bacillus thuringiensis* CryIA(c) toxin, J. Biol. Chem. 270 (1995) 17765–17770.